

ρ -meson properties at finite nuclear density

L. A. Kondratyuk,¹ A. Sibirtsev,² W. Cassing,² Ye. S. Golubeva,³ and M. Effenberger²

¹*Institute of Theoretical and Experimental Physics, 117259 Moscow, Russia*

²*Institute for Theoretical Physics, University of Giessen, D-35392 Giessen, Germany*

³*Institute of Nuclear Research, 117312 Moscow, Russia*

(Received 3 February 1998)

We calculate the momentum dependence of the ρ -meson self-energy based on the dispersion relation for the ρN scattering amplitude $f(\omega)$ at low nuclear density. The imaginary part of $f(\omega)$ is determined from the optical theorem, while the total ρN cross section is obtained within the vector dominance model at high energy and within the resonance model at low energy. Our numerical results indicate a sizable broadening of the ρ -meson width in the medium especially for low relative momenta p while the real part of the ρ self-energy is found to change its sign and to become repulsive already at momenta above 100 MeV/c. Extrapolating to nuclear saturation density ρ_0 we find a dropping of the ρ mass for $p \approx 0$ roughly in line with the QCD sum rule analysis of Hatsuda while at high energy an increase of the ρ mass close to the prediction by Eletsky and Ioffe is obtained. However, when including a broadening of the baryonic resonances in the medium, the ρ -meson mass shift at $p \approx 0$ becomes slightly repulsive, whereas the width increases substantially.

[S0556-2813(98)03308-1]

PACS number(s): 25.20.Dc, 25.40.Ep

I. INTRODUCTION

The properties of baryonic and mesonic resonances in the nuclear medium have received much attention during the last years (see Refs. [1–5]) within the studies on the properties of hot and dense nuclear matter. Here, QCD inspired effective Lagrangian models [1,4,5] or approaches based on QCD sum rules [2,3] predict that the masses of the vector mesons ρ and ω should decrease with the nuclear density. On the other hand, with a dropping hadron mass the phase space for its decay decreases, which results in a modification of its width or lifetime in matter, while due to interactions with the surrounding nuclear medium the resonance width will increase [6–9].

The in-medium properties of vector mesons have been addressed experimentally so far by dilepton measurements at the SPS, both for proton-nucleus and nucleus-nucleus collisions [10–13]. As proposed by Li *et al.* [14], the enhancement in S + Au reactions compared to p + Au collisions in the invariant mass range $0.3 \leq M \leq 0.7$ GeV might be due to a shift of the ρ meson mass. The microscopic transport studies in Refs. [15–17] for these systems point in the same direction, however, more conventional self-energy effects cannot be ruled out at the present stage [15,18–20]. Especially the p -wave coupling of the ρ meson to nucleons induces an attractive interaction at low relative momenta [20] which turns repulsive at large momenta. The explicit momentum dependence of the ρ -meson self-energy thus is an important aspect to be investigated both theoretically and experimentally, e.g., by $\pi^- A$ reactions [8,9,21,22].

The main goal of this paper is to calculate the explicit momentum dependence of the ρ -meson potential at finite nuclear densities within a dispersive approach that is based on the resonance model at low relative momenta of the ρ with respect to the nucleon at rest and the vector dominance model at high relative momenta following the suggestion by

Eletsky and Ioffe [23]. Our work is organized as follows. In Sec. II we briefly recall the relation between hadron self-energies and the hadron-nucleon scattering amplitude at low density and discuss the dominant interaction mechanisms. In Sec. III we present the related dispersion relations and evaluate the ρN scattering amplitude from the ρ -photoproduction cross section at high energy. At low energy we use a resonance model to determine the ρ - N cross section. The implications for the real and imaginary part of the ρ -meson self-energy at finite nuclear density are presented in Sec. IV while a summary and discussion of open problems concludes this work in Sec. V.

II. HADRONIC RESONANCES IN THE NUCLEAR MEDIUM

The relativistic form of the wave equation describing the propagation of a mesonic resonance R in the nuclear matter is given as (see, e.g., Ref. [9])

$$[-\nabla^2 + M_R^2 - iM_R\Gamma_R + U(\mathbf{r})]\Psi(\mathbf{r}) = E^2\Psi(\mathbf{r}), \quad (1)$$

where $E^2 = \mathbf{p}^2 + M_R^2$ and \mathbf{p} , M_R , and Γ_R are the momentum, mass, and width of the resonance, respectively. The optical potential then is defined as

$$U(\mathbf{r}) = -4\pi f_{RN}(0)\rho_N(\mathbf{r}), \quad (2)$$

where $f_{RN}(0)$ is the forward RN -scattering amplitude and ρ_N is the nuclear density.

It is useful to rewrite Eq. (1) in the form

$$[\nabla^2 + \mathbf{p}^2]\Psi(\mathbf{r}) = [U(\mathbf{r}) - \Delta]\Psi(\mathbf{r}), \quad (3)$$

where

$$\Delta = P^2 - M_R^2 - iM_R\Gamma_R \quad (4)$$

is the inverse resonance propagator in the vacuum. The four-momentum P in Eq. (4) can be defined through the four-momenta of the resonance decay products, i.e.,

$$P = p_1 + p_2 + \dots \quad (5)$$

When the resonance decays inside the nucleus of radius R_A at density ρ_N , the propagator has the form

$$\Delta^* = \Delta + 4\pi f(0)\rho_N = P^2 - M_R^{*2} + iM_R^*\Gamma_R^*, \quad (6)$$

where

$$M_R^{*2} = M_R^2 - 4\pi \text{Re} f(0)\rho_N, \quad (7)$$

$$M_R^*\Gamma_R^* = M_R\Gamma_R + 4\pi \text{Im} f(0)\rho_N. \quad (8)$$

Its spectral function then can be described (in a first approximation) by a Breit-Wigner formula (nonrelativistically) as

$$F(M) = \frac{1}{2\pi} \frac{\Gamma_R^*}{(M - M_R^*)^2 + \Gamma_R^{*2}/4}, \quad (9)$$

which contains the effects of collisional broadening

$$\Gamma_R^* = \Gamma_R + \delta\Gamma \quad (10)$$

with

$$\delta\Gamma = \gamma v \sigma_{RN} \rho_N, \quad (11)$$

and a shift of the meson mass

$$M_R^* = M_R + \delta M_R \quad (12)$$

with

$$\delta M_R = -\gamma v \sigma_{RN} \rho_N \alpha. \quad (13)$$

In Eqs. (11),(13) v is the average resonance velocity with respect to the target at rest, γ is the associated Lorentz factor, ρ_N is the nuclear density while σ_{RN} is the resonance-nucleon total cross section, and $\alpha = \text{Re} f(0)/\text{Im} f(0)$.

The sign of the resonance mass shift depends on the sign of the real part of the forward RN scattering amplitude which again depends on the momentum of the resonance. For example, at low momenta ($p \approx 0$) various authors [1–4] predict a decreasing mass of the vector mesons ρ , ω , and ϕ with the nucleon density, whereas Eletsky and Ioffe have argued recently [23] that the ρ meson should become heavier in nuclear matter at momenta of 2–7 GeV/c. If the ratio α is small—which is actually the case for the reactions considered because many reaction channels are open—the broadening of the resonance will be the main effect. As it was shown in Ref. [24] the account of this effect can also essentially influence the predictions of QCD sum rules [2,3]. Therefore it is useful to perform independent calculations for the real part of the ρN forward scattering amplitude which can also be used at low momenta.

Whereas the ρ -meson spectral function in the nuclear medium has been evaluated in Refs. [5,18,19] in dynamical models by considering its 2π decay mode and taking into account the rescattering of pions on nucleons in the medium,

we here address an approach based on dispersion relations using experimental information on the vacuum scattering amplitude as input as well as on the ρ_N couplings (cf. Ref. [25]). Another important point is that Eqs. (11) and (13) for the collisional broadening and mass shift are valid only at low densities when the resonance-nucleon scattering amplitude inside the nucleus is the same as in the vacuum. A discussion of this point will be presented in Sec. III B explicitly.

III. THE ρ -NUCLEON SCATTERING AMPLITUDE IN VACUUM

Within the framework of the vector dominance model (VDM) the Compton scattering amplitude can be expressed through the ρN , ωN , and ϕN scattering amplitudes as

$$T_{\gamma N}(s, t) = \frac{e^2}{4\gamma_\rho^2} \left[T_{\rho N}(s, t) + \frac{\gamma_\rho^2}{\gamma_\omega^2} T_{\omega N}(s, t) + \frac{\gamma_\rho^2}{\gamma_\phi^2} T_{\phi N}(s, t) \right], \quad (14)$$

where $T_{VN}(s, t)$ is the invariant amplitude for the elastic scattering of the transverse polarized vector meson on the nucleon, $e^2/4\pi$ is the fine-structure constant, $T_{\gamma N}(s, t)$ is the invariant Compton scattering amplitude, and $\gamma_\rho^2/4\pi = 0.55$ [26–28]. According to experimental data [29] the last 2 terms on the right-hand side of Eq. (14) including the ωN and ϕN amplitudes can be neglected as compared to the first term. Then the ρN scattering amplitude can be expressed directly through the Compton amplitude by multiplying the latter by $4\gamma_\rho^2/e^2$; this approach has been adopted by Eletsky and Ioffe in Ref. [23]. We note, however, that the experimental Compton scattering amplitude also contains contributions from the continuum of 2π and $n\pi$ intermediate states at high energy such that Eq. (14) appears questionable. Here we will adopt the experimental results on ρ photoproduction instead which are more closely related to the ρ meson itself (see Sec. III A).

In general, the ρN scattering amplitude $f(\omega, \theta)$, which enters into Eqs. (7),(8) for the resonance mass shift and collisional broadening can be expressed through the invariant scattering amplitude by

$$T_{\rho N}(s, t) = 8\pi \sqrt{s} \frac{p_{\text{c.m.}}}{p_{\text{lab}}} f(\omega, \theta), \quad (15)$$

where $p_{\text{c.m.}}$, p_{lab} are the momenta of the incident particle in the c.m. and laboratory systems, respectively, while θ is the scattering angle in the laboratory frame. Furthermore, the real part of the forward ρN scattering amplitude is related to its imaginary part through the dispersion relation (see Ref. [30])

$$\begin{aligned} \text{Re} f(\omega) = & \text{Re} f(\omega_0) + \frac{2(\omega^2 - \omega_0^2)}{\pi} \\ & \times P \int_{\omega_{\text{min}}}^{+\infty} \frac{d\omega' \omega' \text{Im} f(\omega')}{(\omega'^2 - \omega_0^2)(\omega'^2 - \omega^2)}, \end{aligned} \quad (16)$$

where $\omega = \omega_0$ is a subtraction point and ω_{\min} is the threshold energy. The imaginary part of the forward scattering amplitude $\text{Im } f(\omega)$, furthermore, is related to the total cross section by the optical theorem

$$\text{Im } f(\omega) = \frac{P_{\text{lab}}}{4\pi} \sigma_{\text{tot}}(\omega). \quad (17)$$

Thus the knowledge of the total cross section $\sigma_{\text{tot}}(\omega)$ is sufficient to determine $\text{Re } f(\omega)$ through the dispersion relation (16) once the amplitude is known ‘‘experimentally’’ at the subtraction point ω_0 .

A. The ρN total cross section from photoproduction

Within the VDM one can express the ρN scattering amplitude not only through the Compton scattering amplitude [Eq. (14)] but also through the amplitude for ρ photoproduction as

$$T_{\rho N}(s, t) = \frac{2\gamma_\rho}{e} T_{\gamma N \rightarrow \rho N}(s, t). \quad (18)$$

Furthermore, the ρN total cross section can be related to the differential cross section of the reaction $\gamma p \rightarrow \rho p$ as

$$\sigma_{\rho p}^2 = \frac{\gamma_\rho^2}{4\pi} \frac{64\pi}{\alpha} \frac{1}{1 + \alpha_{\rho p}^2} \left(\frac{q_\gamma}{q_\rho} \right)^2 \frac{d\sigma_{\gamma p \rightarrow \rho p}}{dt} \Big|_{t=0}. \quad (19)$$

Here q_γ and q_ρ are the c.m. momenta of the γN and ρN systems at the same invariant collision energy \sqrt{s} . Furthermore, we assume that the ratio $\alpha_{\rho p}$ of the real to imaginary part of the ρN forward scattering amplitude is small. This assumption is valid at least for energies above 3 GeV [29]. Thus using the ρ photoproduction data from Refs. [26–28] the ρN scattering amplitude is fixed at high energy.

We note that at higher energies one can calculate the total cross section of the ρN interaction also within the quark model (QM), where $\sigma_{\rho N}$ can be expressed in terms of pion-nucleon cross sections as

$$\sigma_{\rho^0 N} = \frac{1}{2} (\sigma_{\pi^- N} + \sigma_{\pi^+ N}), \quad (20)$$

while the πN cross sections can be taken from a Regge fit to the experimental data [31]. Though the additive quark model at first sight appears questionable for Goldstone bosons such as the pions, the cross section $\sigma_{\rho N}$ will turn out practically the same as in the VDM for ρ -meson momenta above 2 GeV/c (see below).

B. The resonance model combined with VDM

If the VDM were valid at all energies we could calculate the mass shift and collisional broadening of the ρ meson in nuclear matter at low densities by inserting Eq. (18) in Eqs. (7) and (8) from Sec. II. However, the VDM is expected to hold only at high energies $\omega > 2$ GeV [32] since at lower energies ($\omega \leq 1-1.5$ GeV) there are a lot of baryonic resonances which couple strongly to the transverse as well as the longitudinal ρ mesons [33]. Therefore at low energies it is necessary to describe the ρN interaction within the frame-

TABLE I. Properties of baryonic resonances coupled to the ρ meson; the subscript on the branching ratios denotes the angular momentum of the ρ meson while the stars indicate the confidence level. In our calculations we discard resonances with only one star C.L.

Resonance	J_R	M_R (MeV)	Γ_R (MeV)	$\rightarrow N\rho$ (%)	C.L.
$S_{11}(1650)$	1/2	1659	173	3_S	****
$S_{11}(2090)$	1/2	1928	414	49_S	*
$D_{13}(1520)$	3/2	1524	124	21_S	****
$D_{13}(1700)$	3/2	1737	249	13_S	*
$D_{13}(2080)$	3/2	1804	447	26_S	*
$G_{17}(2190)$	7/2	2127	547	29_D	****
$P_{11}(1710)$	1/2	1717	478	3_P	*
$P_{11}(2100)$	1/2	1885	113	27_P	*
$P_{13}(1720)$	3/2	1717	383	87_P	*
P_{13}	3/2	1879	498	44_P	***
$F_{15}(1680)$	5/2	1684	139	$5_P, 2_F$	****
$F_{15}(2000)$	5/2	1903	494	$60_P, 15_F$	*
$S_{31}(1620)$	1/2	1672	154	$25_S, 4_D$	**
$S_{31}(1900)$	1/2	1920	263	$5_S, 33_D$	***
$D_{33}(1700)$	3/2	1762	599	8_S	*
$D_{33}(1940)$	3/2	2057	460	35_S	*
$P_{31}(1910)$	1/2	1882	239	10_P	****
$F_{35}(1905)$	5/2	1881	327	86_P	***
F_{35}	5/2	1752	251	22_P	*

work of a resonance model [25,34]. In the following we consider the ρN forward scattering amplitude being averaged over the ρ -meson transverse and longitudinal polarizations.

Experimental information on the baryonic resonances and their coupling to the ρ meson is available for masses below 2 GeV. We saturate the ρN total cross section at low energies by the resonances listed in Table I. For the Breit-Wigner contribution of each resonance we adopt the approach developed by Manley and Saleski [35]. In this model the total ρN cross section is given as a function of the ρ -meson mass m and the invariant collision energy \sqrt{s} as

$$\sigma_{\rho N}(m, \sqrt{s}) = \frac{2\pi}{3q_\rho^2} \sum_R (2J_R + 1) \frac{s \Gamma_{\rho N}^{\text{in}}(m, \sqrt{s}) \Gamma_{\text{tot}}(\sqrt{s})}{(s - M_R^2)^2 + s \Gamma_{\text{tot}}^2(\sqrt{s})}. \quad (21)$$

Here q_ρ denotes the c.m. momentum of the ρN system, J_R the spin of the resonance, M_R the pole mass, and Γ_{tot} the total width as a sum over the partial channels. For the case of an unstable particle in the final channel the partial width has to be integrated over the spectral function of this particle. The energy dependence of the partial width $\Gamma_{\rho N}$ for the decay of each baryonic resonance into the ρN channel, i.e., $R \rightarrow \rho N$, is given by

$$\Gamma_{\rho N}(\sqrt{s}) = \Gamma_{\rho N}(M_R) \frac{g(\sqrt{s})}{g(M_R)}, \quad (22)$$

where $\Gamma_{\rho N}(M_R)$ is the ρN partial width at the resonance pole M_R , while the function $g(\sqrt{s})$ is determined as

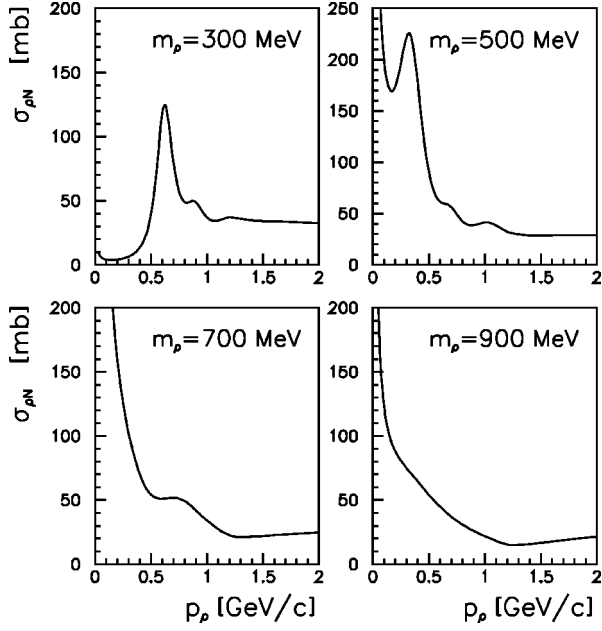


FIG. 1. The total ρN cross section for different invariant masses of the ρ meson. At low energy the cross section was obtained within the resonance model while at high energies it was extrapolated from the quark model (QM) (20).

$$g(\sqrt{s}) = \int_{2m_\pi}^{\sqrt{s}-m_N} A_\rho(m') \frac{q_{\rho N}(m')}{\sqrt{s}} B_l^2(q_{\rho N}) dm'. \quad (23)$$

In Eq. (23) $q_{\rho N}(m')$ is the c.m. momentum of the nucleon and the ρ -meson with mass m' , B_l is a Blatt-Weisskopf barrier penetration factor, l denotes the angular momentum of the ρN system, and A_ρ is the spectral function of the ρ meson in free space taken as

$$A_\rho(m) = \frac{2}{\pi} \frac{m^2 \Gamma_\rho(m)}{(m^2 - M_\rho^2)^2 + m^2 \Gamma_\rho^2(m)}, \quad (24)$$

where $M_\rho = 770$ MeV and the mass-dependent width $\Gamma_\rho(m)$ of the ρ meson is given by

$$\Gamma_\rho(m) = \frac{\Gamma_\rho^0 M_\rho}{m} \left[\frac{q_{\pi\pi}(m)}{q_{\pi\pi}(M_\rho)} \right]^3 \left[\frac{1 + \delta^2 q_{\pi\pi}^2(M_\rho)}{1 + \delta^2 q_{\pi\pi}^2(m)} \right] \quad (25)$$

with $\delta = 5.3$ (GeV/c) $^{-1}$ and $\Gamma_\rho^0 = 150$ MeV.

The incoming width in Eq. (21) reads

$$\Gamma_{\rho N}^{\text{in}}(m, \sqrt{s}) = C_{\rho N}^{I_R} \frac{q_{\rho N}(m)}{\sqrt{s}} B_l^2(q_{\rho N}) \frac{\Gamma_{\rho N}(M_R)}{g(M_R)}, \quad (26)$$

where $C_{\rho N}$ denotes the appropriate Clebsch-Gordan coefficient for the coupling of the isospins of ρ and nucleon to the isospin I_R of the resonance. The properties of the baryonic resonances coupled to the ρ are listed in Table I; in the following calculations we exclude the resonances with only one star confidence level.

Within the resonance model we can evaluate the total ρN cross section as the function of two variables: the ρ momentum and the invariant mass m of the ρ meson. Figure 1

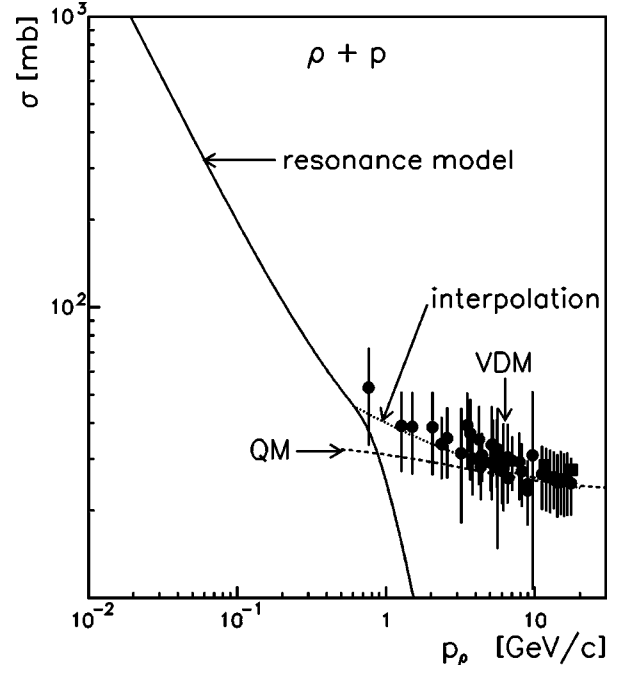


FIG. 2. The total $\rho\rho$ cross section. The solid line shows our calculation within the resonance model (21) while the dashed line is the result from the quark model (QM) (20). The full circles show the experimental data extracted from ρ photoproduction while the squares are from Ref. [36]. The dotted line indicates the interpolation that will be used further on.

shows the momentum dependence of the total ρN cross section according to Eq. (21) for different masses of the ρ -meson. At higher momenta ($p_\rho \geq 1.5$ GeV/c), where the total cross section is described by the VDM or the QM (20), respectively, we assume that it no longer depends on m .

In Fig. 2 we present the prediction of the resonance model for the total $\rho\rho$ cross section—averaged over the ρ -meson spectral function A_ρ —in comparison with the result from the quark model (20) (QM, dashed line). The solid circles in Fig. 2 show the total $\rho\rho$ cross section obtained by Eq. (19) and the experimental forward ρ -photoproduction data from Refs. [26–28]. Furthermore, the squares in Fig. 2 (for $p_\rho \geq 10$ GeV/c) show the ρN cross section extracted from the reaction $\gamma + d \rightarrow \rho^0 + d$ independently of the VDM [36]. As mentioned before, the results for the total cross section of the ρN interaction calculated within the framework of the quark model and the VDM are in fair agreement at momenta above 2 GeV/c. The dotted line in Fig. 2 shows the interpolation between the low- and high-energy parts of the total $\rho\rho$ cross section which we will adopt further on in Eq. (17).

In order to compute the real part of the amplitude we use the dispersion relation (16) and perform the subtraction at $\omega_0 = 4.46$ GeV since at this energy $\text{Re } f(\omega_0)$ was calculated with the VDM from the ρ -meson photoproduction differential cross section measured by DESY-MIT [37] and the Daresbury group [38]. We note that the VDM should be valid at the energy of 4.46 GeV such that the subtraction point is no hidden parameter in our approach. Since the resonance model is also valid below the ρN threshold, the ρ contribution in this case is calculated as an integral over the available invariant mass of the 2π system.

The real and imaginary parts of the $f_{\rho N}$ amplitude—

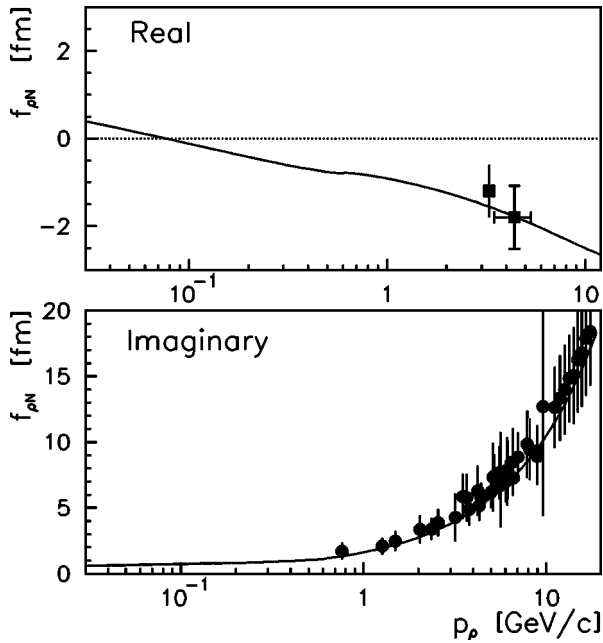


FIG. 3. Real and imaginary part of the ρN scattering amplitude in free space from the calculations (solid lines). The circles and squares are the results evaluated from the experimental data for ρ -meson photoproduction.

calculated with the total ρN cross section averaged over the ρ -meson spectral function in free space (24)—are shown in Fig. 3. The imaginary part corresponds to the total $\rho\rho$ cross section from Fig. 2 using the dashed line as an interpolation. Whereas the real part $\text{Re } f_{\rho N}$ is negative at high momentum, it changes sign at $p_\rho \approx 100$ MeV/ c . This behavior of the real part for the $f_{\rho N}$ amplitude has its origin in the resonance contribution at low energies. To illustrate this point we present in Fig. 4 $\text{Re } f_{\rho N}$ neglecting the part of the ρN cross section from the resonance model. In fact, in this case the real part does not change its sign and remains negative over the whole momentum range.

Furthermore, Fig. 5 shows the real part of the forward ρN scattering amplitude calculated for the different masses of the two-pion system m coupled to the ρ meson. We find that $\text{Re } f_{\rho N}$ substantially depends on the ρ -meson mass as well as on momentum. Note that the dip for $p_\rho \approx 1$ GeV/ c is due to our interpolation between the low- and high-energy regions and thus an artifact of our model which should be discarded. We also have to mention that the magnitude of the ρ -meson momentum, where the real part of the forward ρN scattering amplitude changes its sign, depends on the prescription for the transition between the resonance and the high-energy part of the total cross section, which is actually model dependent, and estimate this uncertainty as $\delta p_\rho = \pm 30$ MeV/ c .

IV. MASS SHIFT AND BROADENING OF THE ρ MESON IN THE NUCLEAR MEDIUM

In the low density approximation one now can express the correction of the ρ -meson mass and width at finite nuclear density ρ_N through $f_{\rho N}$ using Eqs. (7) and (8). We show the corresponding results for the mass and width of the ρ meson

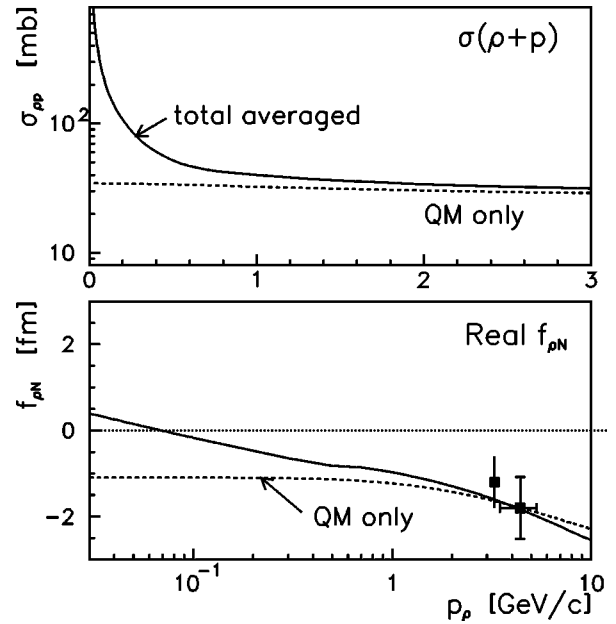


FIG. 4. The total $\rho\rho$ cross section and the real part of the ρN scattering amplitude in free space as a function of the momentum p_ρ . The solid lines show our calculations with the total ρN cross section while the dashed lines indicate the results with the cross section from the quark model (20), only. The squares are evaluated from the experimental data for ρ -meson photoproduction.

in Fig. 6 calculated at saturation density $\rho_0 \approx 0.16$ fm $^{-3}$ with the averaged ρN cross section from the resonance model as described above. The upper part of Fig. 6 also shows the recent result from Hatsuda [39] calculated within the QCD sum rule approach at $\omega = m_\rho$ by the full dot. Our

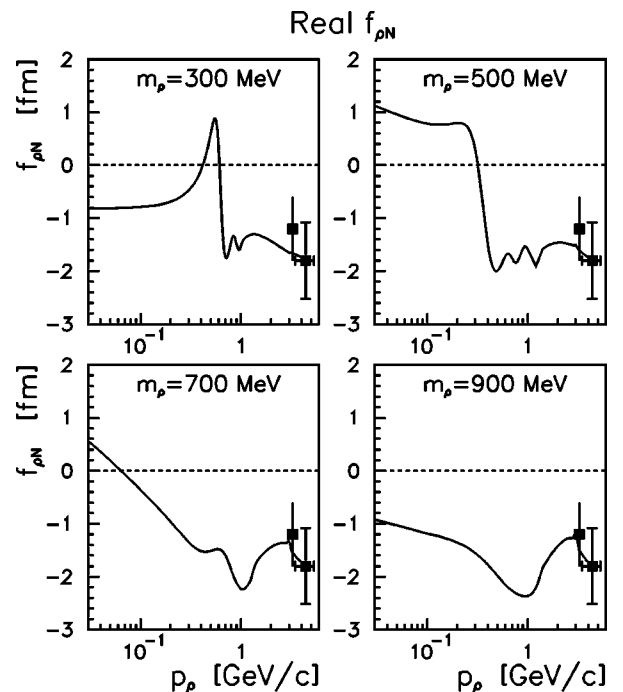


FIG. 5. The real part of the ρN scattering amplitude in free space calculated for different masses of the ρ meson. The squares are evaluated from the experimental data for ρ -meson photoproduction.

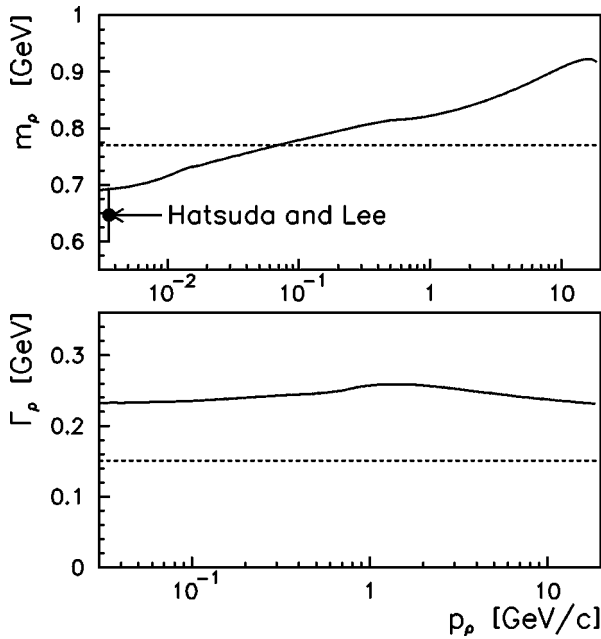


FIG. 6. Mass and width of the ρ meson at $\rho_N=0.16 \text{ fm}^{-3}$ according to our model in the low density approximation. The full dot corresponds to the result from Hatsuda [39] within the QCD sum rule approach.

result for δm in the low density approximation is in agreement with this calculation for $p_\rho \approx 0$. Note that the QCD sum rule analysis is also limited to low nuclear densities due to the unknown behavior of the quark four-point condensates in the medium. At high momenta $p \geq 2 \text{ GeV}/c$ our result is also in qualitative agreement with the VDM predictions for the mass shift as found by Eletsky and Ioffe [23]. In their case the ρ mass shift increases from 60 MeV at $p_\rho = 2 \text{ GeV}/c$ to 90 MeV at $7 \text{ GeV}/c$, whereas our analysis gives a shift of $\approx 70 \text{ MeV}$ at $2 \text{ GeV}/c$ and $\approx 120 \text{ MeV}$ at $7 \text{ GeV}/c$. The deviations with the results from Ref. [23] are due to the use of the ρ -photoproduction amplitudes (19) instead of the Compton scattering amplitude (14) used by the latter authors.

Thus, if the low density approximation could be extrapolated up to ρ_0 , our model would demonstrate that the repulsive interaction of the ρ meson at high momenta might be consistent with an attractive ρN interaction at low energies. However, as it was shown in Ref. [24], the effect of the finite ρ width can essentially influence the predictions of QCD sum rules [2,3]. Furthermore, recent microscopic calculations of the ρ -spectral function at low energies do not show any substantial attraction for slow ρ mesons at normal nuclear density [5,40].

It is thus important to check if the results obtained within the low density approximation are still valid at normal nuclear density ρ_0 . Up to now in calculating the mass shift and broadening of the width for the ρ meson (shown in Fig. 6) we have used the vacuum ρN scattering amplitude with resonance contributions which, however, might be different in nuclear matter. An indication for a possible strong medium modification of baryonic resonances is the experimental observation that the total photoabsorption cross section in nuclei for $A \geq 12$ does not show any resonant structure except the $\Delta(1232)$ isobar [41–43]. As was shown in Refs.

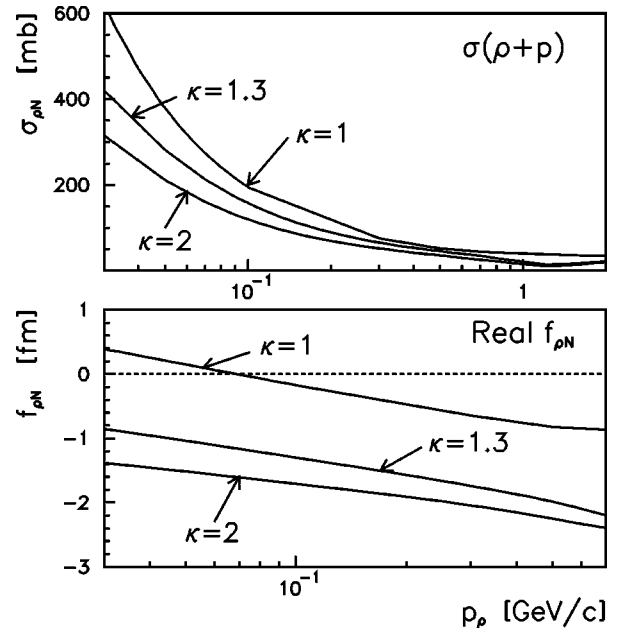


FIG. 7. The total ρN cross section and the real part of the ρN scattering amplitude calculated for different widths of the baryonic resonances. The factor κ indicates the ratio of the in-medium resonance width to its vacuum width.

[6,44] this might be explained by a strong in-medium broadening of the $D_{13}(1520)$ resonance ($\Gamma_{\text{med}} \approx 300 \text{ MeV}$ compared to the vacuum width $\Gamma_R \approx 120 \text{ MeV}$), but not by conventional medium effects such as Fermi motion or Pauli blocking. While a collision broadening of this order is hard to justify, it might arise from the strong coupling of the D_{13} resonance to the ρN channel and a medium modification of the ρ meson [34]. Furthermore, in Ref. [40] it has been shown that such a mechanism can lead to an in-medium width of the $D_{13}(1520)$ resonance of about 350 MeV.

To estimate how the latter effect influences our results we have performed also calculations for the in-medium ρN total cross section by assuming that at normal nuclear density the widths of all resonances—coupled to the ρN channel—are twice as in the vacuum, but their ρN branching ratios stay the same. This in-medium ρN cross section then was used in the dispersion relation for the calculation of the in-medium real part of the ρN forward scattering amplitude.

The results of these calculations are shown in Fig. 7 for the total ρp cross section and the real part of the forward scattering amplitude calculated with different widths of all baryonic resonances. The factor κ in Fig. 7 stands for the ratio of the in-medium width of the baryonic resonance to its value in free space. We see that the higher order resonance broadening effects have a strong influence on the ρN scattering amplitude in the resonance region. The total cross section becomes smoother at low energy and as a result the real part of $f_{\rho N}(0)$ does not change sign anymore with decreasing p_ρ . At small p_ρ it remains negative, which means that the main medium effect for the ρ meson at normal nuclear density is the collisional broadening; the mass shift is slightly repulsive. This result is in qualitative agreement with recent calculations of the ρ -meson spectral function at low energies from Refs. [5,18,40]. However, a note of caution has to be added here because the predictions within the reso-

nance model are only of qualitative nature. The properties of nuclear resonances as well as their branching to the ρ channel in the dense medium are unknown so far. Furthermore, the influence of exchange-current corrections at high density on the ρ -meson properties should be considered as well.

V. CONCLUSIONS

In summary, we have calculated the momentum dependence of the ρ -meson self-energy (or in-medium properties) based on the dispersion relation (16) for the ρN scattering amplitude at finite (but small) nuclear density. The imaginary part of $f(\omega)$ is calculated via the optical theorem (17) while the total ρN cross section is obtained within the VDM at high energy and within the resonance model at low energy. The scattering amplitude $f(\omega)$ thus is entirely based on experimental data. Our numerical results indicate a sizable broadening of the ρ -meson width in the medium especially for low relative momenta p_ρ . In the low density approximation the real part of its self-energy is found to be attractive for $p_\rho \leq 100$ MeV/c and to change its sign, becoming repulsive at higher momenta in line with the prediction by Eletsky and Joffe [23]. Extrapolating the low density approximation to nuclear saturation density we obtain a dropping of the ρ mass at $p_\rho \approx 0$ in line with the QCD sum rule analysis of Hatsuda [39]. Thus our dispersion approach demonstrates that the results of Refs. [23] and [39] do not contradict each

other due to the rather strong momentum dependence of the ρN scattering amplitude.

However, the resonance part of the ρN scattering amplitude is also influenced by the nuclear medium at saturation density such that the moderate attraction at $p_\rho \approx 0$ changes to a small repulsion. This behavior of the ρ -meson self-energy is in qualitative agreement with the recent microscopic calculations of Rapp, Chanfray, and Wambach [18,19] as well as Klingl *et al.* [5] for the ρ spectral function. In the latter case the ρ meson essentially broadens significantly in the dense medium which implies lifetimes of the ρ meson of less than 1 fm/c already at density ρ_0 ; in simple words, according to our dispersion approach the ρ meson “melts” at high nuclear density and does not “drop in mass” as suggested by the scaling hypothesis of Ref. [1]. We note, finally, that the explicit momentum dependence of the ρ -meson self-energy is also an important issue that has to be incorporated, e.g., in transport theories that attempt to extract information on the ρ spectral function in comparison to experimental dilepton data.

ACKNOWLEDGMENTS

The authors acknowledge many helpful discussions with K. Boreskov, E. L. Bratkovskaya, B. L. Ioffe, U. Mosel, and Yu. Simonov throughout this study. This work was supported by DFG, Forschungszentrum Jülich, and BMBF.

-
- [1] G. E. Brown and M. Rho, Phys. Rev. Lett. **66**, 2720 (1991).
 - [2] T. Hatsuda and S. Lee, Phys. Rev. C **46**, R34 (1992).
 - [3] M. Asakawa and C. M. Ko, Phys. Rev. C **48**, R526 (1993).
 - [4] C. M. Shakin and W.-D. Sun, Phys. Rev. C **49**, 1185 (1994).
 - [5] F. Klingl and W. Weise, Nucl. Phys. **A606**, 329 (1996); F. Klingl, N. Kaiser, and W. Weise, *ibid.* **A617**, 449 (1997); **A624**, 927 (1997).
 - [6] L. A. Kondratyuk, M. Krivoruchenko, N. Bianchi, E. De Sanctis, and V. Muccifora, Nucl. Phys. **A579**, 453 (1994).
 - [7] K. G. Boreskov, J. Koch, L. A. Kondratyuk, and M. I. Krivoruchenko, Phys. At. Nucl. **59**, 1908 (1996); K. G. Boreskov, L. A. Kondratyuk, M. I. Krivoruchenko, and J. Koch, Nucl. Phys. **A619**, 295 (1997).
 - [8] W. Cassing, Ye. S. Golubeva, A. S. Iljinov, and L. A. Kondratyuk, Phys. Lett. B **396**, 26 (1997).
 - [9] Ye. S. Golubeva, L. A. Kondratyuk, and W. Cassing, Nucl. Phys. **A625**, 832 (1997).
 - [10] G. Agakichiev *et al.*, Phys. Rev. Lett. **75**, 1272 (1995).
 - [11] M. A. Mazzoni, Nucl. Phys. **A566**, 95c (1994).
 - [12] T. Åkesson *et al.*, Z. Phys. C **68**, 47 (1995).
 - [13] A. Drees, Nucl. Phys. **A610**, 536c (1996).
 - [14] G. Q. Li, C. M. Ko, and G. E. Brown, Phys. Rev. Lett. **75**, 4007 (1995).
 - [15] W. Cassing, W. Ehehalt, and C. M. Ko, Phys. Lett. B **363**, 35 (1995).
 - [16] W. Cassing, W. Ehehalt, and I. Kralik, Phys. Lett. B **377**, 5 (1996).
 - [17] E. L. Bratkovskaya and W. Cassing, Nucl. Phys. **A619**, 413 (1997).
 - [18] R. Rapp, G. Chanfray, and J. Wambach, Phys. Rev. Lett. **76**, 368 (1996).
 - [19] R. Rapp, G. Chanfray, and J. Wambach, Nucl. Phys. **A617**, 472 (1997).
 - [20] B. Friman and H. J. Pirner, Nucl. Phys. **A617**, 496 (1997).
 - [21] W. Schön, H. Bokemeyer, W. Koenig, and V. Metag, Acta Phys. Pol. B **27**, 2959 (1996).
 - [22] Th. Weidmann, E. L. Bratkovskaya, W. Cassing, and U. Mosel, nucl-th/971104.
 - [23] V. L. Eletsky and B. L. Ioffe, Phys. Rev. Lett. **78**, 1010 (1997).
 - [24] S. Leupold, W. Peters, and U. Mosel, Nucl. Phys. **A628**, 311 (1998).
 - [25] A. Sibirtsev and W. Cassing, Nucl. Phys. **A629**, 707 (1998).
 - [26] R. Anderson, D. Gustavson, J. Johnson, D. Ritson, B. H. Wiik, W. G. Jones, D. Kreinick, F. Murphy, and R. Weinstein, Phys. Rev. D **1**, 27 (1970).
 - [27] J. Ballam *et al.*, Phys. Rev. D **7**, 3150 (1973).
 - [28] R. M. Eglhoff *et al.*, Phys. Rev. Lett. **43**, 657 (1979).
 - [29] T. H. Bauer, R. D. Spital, D. R. Yennie, and F. M. Pipkin, Rev. Mod. Phys. **50**, 261 (1978).
 - [30] J. D. Bjorken and S. D. Drell, *Relativistic Quantum Fields* (McGraw-Hill, New York, 1965), p. 209.
 - [31] A. Donnachie and P. V. Landshoff, Phys. Lett. B **296**, 227 (1992).
 - [32] B. L. Ioffe, V. A. Khoze, and L. N. Lipatov, *Hard Processes* (North-Holland, Amsterdam, 1984), Vol. 1.
 - [33] Particle Data Group, R. M. Barnett *et al.*, Phys. Rev. D **54**, 1 (1996).

- [34] M. Effenberger, A. Hombach, S. Teis, and U. Mosel, Nucl. Phys. **A613**, 353 (1997); **A614**, 501 (1997).
- [35] D. M. Manley and E. M. Saleski, Phys. Rev. D **45**, 4002 (1992).
- [36] R. L. Anderson, D. Gustavson, J. Johnson, I. Overman, D. M. Ritson, and B. H. Wiik, Phys. Rev. D **4**, 3245 (1971).
- [37] H. Alvensleben *et al.*, Phys. Rev. Lett. **25**, 1377 (1970); **27**, 444 (1971).
- [38] P. J. Biggs, D. W. Braben, R. W. Clift, E. Gabathuler, and R. E. Rand, Phys. Rev. Lett. **27**, 1157 (1971).
- [39] T. Hatsuda, nucl-th/9702002.
- [40] W. Peters, M. Post, H. Lenske, S. Leupold, and U. Mosel, Nucl. Phys. **A632**, 109 (1998).
- [41] N. Bianchi *et al.*, Phys. Lett. B **299**, 219 (1993); **309**, 5 (1993); **325**, 333 (1994); M. Anghinolfi *et al.*, Phys. Rev. C **47**, R922 (1993).
- [42] N. Bianchi *et al.*, Phys. Rev. C **54**, 1688 (1996).
- [43] Th. Frommhold, F. Steiper, W. Henkel, U. Kneissl, J. Ahrens, R. Beck, J. Peise, and M. Schmitz, Phys. Lett. B **295**, 28 (1992).
- [44] S. Boffi, Y. Golubeva, L. A. Kondratyuk, M. I. Krivoruchenko, and E. Perazzi, Phys. At. Nucl. **60**, 1193 (1997).